False Color Fusion for Multi-band SAR Images Based on Contourlet Transform

ZHENG Yong-An[1] SONG Jian-She[1] ZHOU Wen-Ming[1] WANG Rui-Hua[1]

Abstract A false color image fusion method for multi-band synthetic aperture radar (SAR) images based on contourlet transform is presented. It works in the following way: firstly, the flexible multiresolution, high directionality and anisotropy of contourlet transform are used for implementing the multiscale decomposition for SAR images. In the contourlet transform domain, an edge information measurement rule is used to merge the directional subbands, and an averaging rule is used to merge the lowpass subbands. Then, a hybrid high boost filter algorithm is proposed to produce the red, green and blue color channels of red-green-blue (RGB) model based on the gray fused image. Finally, the false color fused image is displayed in the RGB color space. This method translates the gray information into color information available to human visual system and enhances the spectral resolution for SAR images. Experimental results is confirmed the validity of the proposed method.

Key words Contourlet transform, false color fusion, hybrid high boost

1 Introduction

Synthetic aperture radar (SAR) are active microwave remote sensors that possess the advantages of all-time, all-weather, high-resolution and long distance imagery. It has been widely used in the field of remote sensing, military detection and earth observation. As the electromagnetic waves are different, the different band SAR images may present different image characteristics for the same scene. The shorter band SAR images can offer the outside scenes and the image characteristics are close to those of optical images. Otherwise, the longer band SAR images may offer the scene of the underground targets. The gray fusion of different bands SAR images can merge the complementary information. SAR images only have gray information and some details are difficult to be distinguished by human eyes. False color fusion can translate gray into colors well suited for human eyes and it will also be available for further target recognition and classification. The fusion of multi-band SAR images should provide the "stereo scene" and "full scene" of images and enhance the detecting capability of the SAR system.

Over the last two decades, wavelets have had a growing impact on image fusion, mainly due to their good non-linear approximation performance for piecewise smooth functions in one dimension[1]. Unfortunately, this is not the case in two dimensions. In essence, wavelets are good at catching point or zero-dimension discontinuities. Intuitively, wavelets in 2-D obtained by a tensor-product of one dimensional wavelets will be good at isolating the discontinuities at edge points, but will not be able to see the smoothness along the contours[2].

The new developed contourlet[2,3] can solve the problem of multi-dimension discontinuities expansion. It exhibits high directional sensitivity and high anisotropy and can exactly capture the image edges to the different scale and frequency subbands. It has been used for image denoising[4], compression[5] and fusion[6] and is well suitable for the fusion of multi-band SAR images that possess a much larger amount of texture information than wavelets.

A false color fusion method based on the gray fused result in the contourlet domain is presented in the paper. To merge two bands SAR images, an edge information measurement rule is employed to merge the directional high-frequency subbands decomposed by contourlets. Then the hybrid high boost filter algorithm is used between the fused gray images and the original images. The filtered results are presented through red, green and blue channels of RGB color space, respectively. Finally the fused result is displayed with the false color.

Received November 10, 2006; in revised form December 14, 2006
Supported by National Natural Science Foundation of P. R. China (60272022)
1. Xi′an Research Institute of High-tech, Xi′an 710025, P. R. China
DOI: 10.1360/aas-007-0337

2 Gray image fusion based on contourlet transform

2.1 Contourlet transform

Contourlets were constructed based on the filter bank theory in the discrete domain and it was a double filter bank approach for obtaining sparse expansions for typical images with smooth contours. In the constructed pyramidal directional filter bank (PDFB), the Laplacian pyramid (LP) was first used to capture the point discontinuities, and then a directional filter bank (DFB) was used to link point discontinuities into linear structures. The multi-scale decomposition and the directional decomposition are two independent processes. The overall result was an image expansion using basic elements like contour segments. In particular, contourlets have elongated supports at various scales, directions, and aspect rations, offering a flexible multiresolution and directional decomposition for images, since they allow for a different number of directions at each scale. A briefly construction of contourlet transform is shown in Fig. 1.

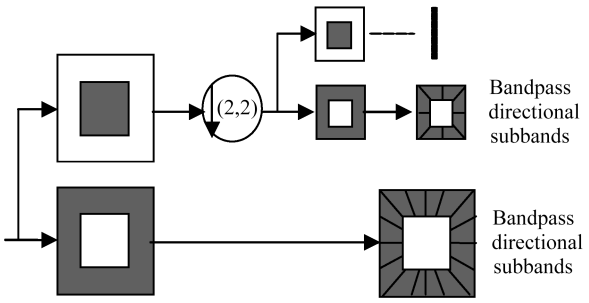

Fig. 1 The construction of contourlet transform

Associated with the LP is a multiscale decomposition of the $L^2(\mathcal{R}^2)$ space into a series of increasing resolutions.

$$L^2(\mathcal{R}^2) = V_{j_0} \oplus (\bigoplus_{j=j_0}^{-\infty} W_j) \quad (1)$$

According to the definition of the subspaces V_{j_0} and W_j as in the wavelet multiresolution analysis, V_{j_0} is an approximation subspace at the scale 2^{j_0}, whereas W_j contains the added details to the finer scale 2^{j-1}. In the LP, each subspace W_j is spanned by a frame $\{\mu_{j,n}(t)\}_{n\in\mathcal{Z}^2}$ that assimilates a uniform grid on $\mathcal{R}^2$ at intervals $2^{j-1}\times 2^{j-1}$.

For the directional filter bank, it can be shown that an l-level DFB generates a local directional basis for $L^2(\mathcal{Z}^2)$ that is composed of the impulse responses of the 2^l directional filters and their shifts.

$$\{g_k^{(l)}[\cdot - S_k^{(l)}n]\}_{0\le k<2^l, n\in\mathcal{Z}^2} \tag{2}$$

where the sampling matrices have the following two forms, depending on whether the representing directional is "nearly horizontal" or "nearly vertical"

$$S_k^{(l)} = \begin{cases} \begin{bmatrix} 2^{l-1} & 0 \\ 0 & 2 \end{bmatrix} & 0\le k<2^{l-1} \\ \begin{bmatrix} 2 & 0 \\ 0 & 2^{l-1} \end{bmatrix} & 2^{l-1}\le k<2^l \end{cases} \tag{3}$$

In the contourlet transform, suppose that an l_j-level DFB is applied to the detail subspace W_j of the LP. This results in a decomposition of W_j into 2^{l_j} directional subspaces at scale 2^j.

$$W_j = \bigoplus_{k=0}^{2^{l_j}-1} W_{j,k}^{(l_j)} \tag{4}$$

Each subspace $W_{j,k}^{(l_j)}$ is spanned by a frame $\{\rho_{j,k,n}^{(l_j)}(t)\}_{n\in\mathcal{Z}^2}$ with a redundancy ratio equal to 4/3, where

$$\rho_{j,k,n}^{(l_j)}(t) = g_k^{(l_j)}[m - S_k^{(l_j)}n]\mu_{j,m}(t) \tag{5}$$

Furthermore, $\{\rho_{j,k,n}^{(l_j)}(t)\}_{n\in\mathcal{Z}^2}$ is generated from a single prototype function and its shifts:

$$\rho_{j,k,n}^{(l_j)}(t) = \rho_{j,k}^{(l_j)}(t - 2^{j-1}S_k^{(l_j)}n), \quad n\in\mathcal{Z}^2 \tag{6}$$

As a result, the $W_{j,k}^{(l_j)}$ is a shift invariant space defined on a rectangular grid of interval $2^{j+l_j-2}\times 2^j$(or $2^j\times 2^{j+l_j-2}$, just depending on whether the representing direction is nearly horizontal or nearly vertical). Do and Vetterli[7,8] refer to function $\{\rho_{j,k,n}^{(l_j)}(t)\}_{n\in\mathcal{Z}^2}$ as contourlets. The indexes j, k, and n are for the scale, direction, and location, respectively. Fig. 2 illustrates the 3-level contourlet decomposition for Zoneplate image.

2.2 Gray image fusion in contourlet domain

Multiscale contourlet transform has been employed to decompose the registered multi-band SAR images (*e.g.* two different band images A and B). Firstly, LP is utilized to decompose images into lowpass coefficients $\{S_l^A(i,j), l = 1,2,\cdots,N\}$, $\{S_l^B(i,j), l = 1,2,\cdots,N\}$ and bandpass coefficients $\{D_l^A(i,j), l = 1,2,\cdots,N\}$, $\{D_l^B(i,j), l = 1,2,\cdots,N\}$, where l is the scale. Then DFB is employed such that bandpass coefficients can implement the directional decomposition. Let $\{D_l^A(i,j,k_l), l = 1,2,\cdots,N\}$ and $\{D_l^B(i,j,k_l), l = 1,2,\cdots,N\}$ denote the coefficients of DFB, where k_l is the directional numbers of l-level bandpass coefficients. As the multiscale decomposition and the directional decomposition are separable, the directional numbers of any level can be different, but when fusing, the directional numbers of the two original images must be the same.

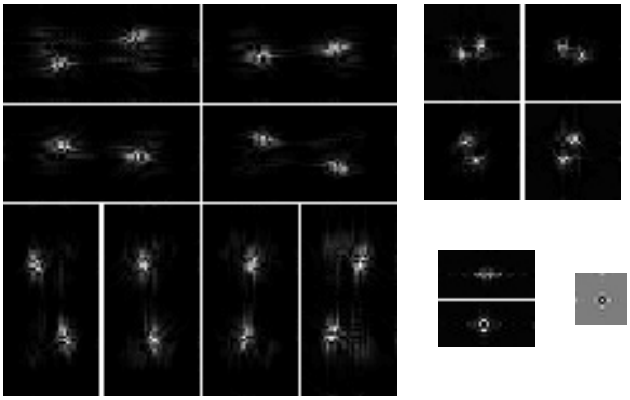

Fig. 2 The directional subbands and lowpass subband of 3 levels contourlet decomposition for Zoneplate image

Firstly, the averaging rule is adopted for lowpass coefficients fusion. Let $\{S_l^F(i,j), l = 1,2,\cdots,N\}$ be the fused lowpass coefficients. Then

$$S_l^F(i,j) = (S_l^A(i,j) + S_l^B(i,j))/2 \tag{7}$$

Then an edge information measurement (EIM) based on regional windows is defined as a threshold for directional high-frequency coefficients[9]. Let $M_l^A(i,j,k_l)$ and $M_l^B(i,j,k_l)$ denote the EIM. Then

$$M_l^\varepsilon(i,j,k_l) = \sum_s\sum_t w(s,t)D_l^\varepsilon(i+s,j+t,k_l) \tag{8}$$

where $\varepsilon = A$ or B , denoting different original images.

$$w(s,t) = \begin{bmatrix} -1 & -1 & -1 \\ -1 & 8 & -1 \\ -1 & -1 & -1 \end{bmatrix} \tag{9}$$

$w(s,t)$ is the Laplacian edge detection mask. If the fused directional high-frequency coefficients are $D_l^F(i,j,k_l), l = 1,2,\cdots,N$, then

$$D_l^F(i,j,k_l) = \begin{cases} D_l^A(i,j,k_l) & \text{if} \quad M_l^A(i,j,k_l) > M_l^B(i,j,k_l) \\ D_l^B(i,j,k_l) & \text{if} \quad M_l^A(i,j,k_l) \le M_l^B(i,j,k_l) \end{cases} \tag{10}$$

Probabilistic consistency verification must be implemented for fused coefficients. If 6 or more than 6 out of 8 neighborhoods pixels for a center pixel come from image A, then the center pixel is decided by A, otherwise it is decided by B. Finally, the inverse contourlet transform is employed to reconstruct the fused image with fused lowpass coefficients and directional high-frequency coefficients.

The registered Ku band and L band SAR images about the same scene offered by the 38th Research Institute of CETC have been utilized to implement the fusion experiments. The fused results are shown in Fig. 3

3 Hybrid high boost filtered false color fusion

The gray information resolving power of human visual system has limitations. The false color fusion can trans-

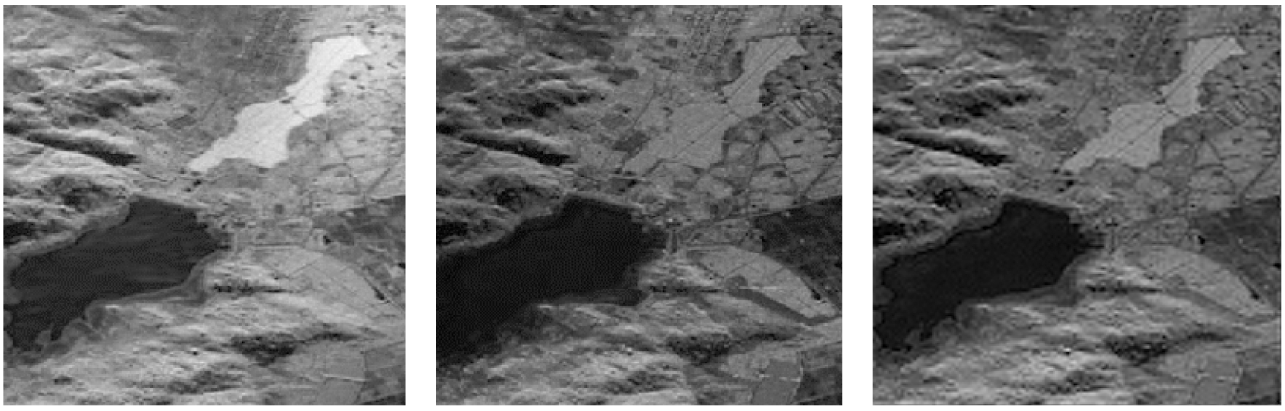

Fig. 3 Gray fusion of multi-band SAR images. (a) Original Ku band SAR image. (b) Original L band SAR image. (c) Contourlet-based gray fused image.

late the gray information into easily distinguishable color information. In order to display the fused result in false color spaces, three color channels of RGB color model are needed. The high boost filtered result of the gray fused image in the contourlet domain was proposed to serve as a color channel, and a hybrid high boost filter algorithm was applied to generate the two other color channels. Let I_{hb} denote the high boost filtered image of the input image I, where

$$\begin{aligned} I_{hb} &= \alpha \cdot I_{original} + I_{highpass} \\ &= (\alpha \cdot W_{allpass} + W_{highpass}) I_{original} \\ &= W_{hb} I_{original} \end{aligned} \tag{11}$$

Then $W_{highboost} = \alpha \cdot W_{allpass} + W_{highpass}$ is a high boost convolution kernel and $\alpha > 0$ is a constant.

$$\begin{aligned} W_{hb} &= \alpha \cdot W_{allpass} + W_{highpass} \\ &= \alpha \begin{bmatrix} 0 & 0 & 0 \\ 0 & 1 & 0 \\ 0 & 0 & 0 \end{bmatrix} + \begin{bmatrix} 0 & -1 & 0 \\ -1 & 4 & -1 \\ 0 & -1 & 0 \end{bmatrix} \\ &= \begin{bmatrix} 0 & -1 & 0 \\ -1 & \alpha+4 & -1 \\ 0 & -1 & 0 \end{bmatrix} \end{aligned} \tag{12}$$

or

$$\begin{aligned} W_{hb} &= \alpha \cdot W_{allpass} + W_{highpass} \\ &= \alpha \begin{bmatrix} 0 & 0 & 0 \\ 0 & 1 & 0 \\ 0 & 0 & 0 \end{bmatrix} + \begin{bmatrix} -1 & -1 & -1 \\ -1 & 8 & -1 \\ -1 & -1 & -1 \end{bmatrix} \\ &= \begin{bmatrix} -1 & -1 & -1 \\ -1 & \alpha+8 & -1 \\ -1 & -1 & -1 \end{bmatrix} \end{aligned} \tag{13}$$

High boost filter algorithm can enhance the high frequency information while preserving the low frequency information. According to [10], equation (11) can be modified into

$$I_{hb} = \alpha \cdot I_{original} + \beta \cdot I_{highpass} \tag{14}$$

where $\alpha > 0$, $\beta > 0$ are constants and can be adjusted to satisfy the image enhancement. As the contourlet-based gray fused image integrates the features of the two original images, the fused image is strongly correlative with the original images. To define a hybrid high boost filter algorithm between the fused images and original images to generate the other two color channels, we let F denote the gray fused images. Then the hybrid high boost filtered image can be obtained from the following two equations:.

$$AF_{hb}(i,j) = \alpha \cdot A(i,j) + \beta \cdot F_{highpass}(i,j) \tag{15}$$

$$BF_{hb}(i,j) = \alpha \cdot B(i,j) + \beta \cdot F_{highpass}(i,j) \tag{16}$$

Put $\{AF_{hb}, F_{hb}, BF_{hb}\}$ to the three color channels of RGB model and display it in false color space. Fig. 4 illustrates the false color images. Fig. 4 (a) is the high boost filtered image of the gray fused image. Fig. 4 (b) and Fig. 4 (c) are the hybrid high boost filtered images of the gray fused image and two original images. Fig. 4 (d) illustrates the false color fused image of the proposed method and Fig. 4 (e) is the fused image of false color mapping[10].

The false color images of the two methods have integrated the information of the original images (Fig.4). Some details that are difficult to distinguish in the original gray images can be easily discriminated after it occupies the color. In order to make a visual contrast between the two fused images, the images have been locally modified two times as shown in Fig. 4 (f). The upper image of Fig. 4 (f) is the magnified result of the proposed method and neither image is the magnified result of false color mapping method. It can be seen that the color of the fused image has more balance and it suits for human visual system. Obvious block phenomena occur in the result of false color mapping and the fused image is distorted.

4 Objective evaluation

Standard deviation, entropy, mean gradient and correlation coefficient[11,12] have been used to make a quantitative evaluation of the fused results. The standard deviation (STD) is defined as

$$STD = \sqrt{\frac{1}{MN-1} \sum_{i=1}^{M} \sum_{j=1}^{N} (I(i,j) - \bar{I})^2} \tag{17}$$

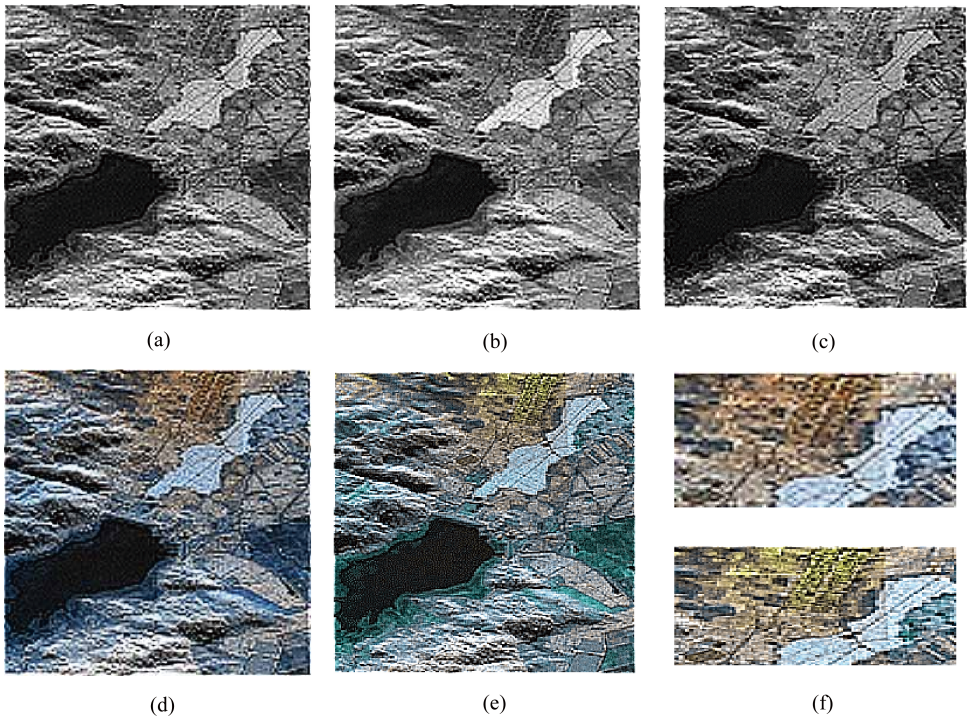

Fig. 4 The false color fused results of multi-band SAR images($\alpha = 2.0, \beta = 1.0$). (a) High boost filter of the gray fused image. (b) Hybrid high boost filter between the gray fused image and the original image A. (c) Hybrid high boost filter between the gray fused image and the original image B. (d) The fused image with the proposed method. (e) The fused image of the false color mapping method. (f) The images of locally magnify 2 times.

where M and N are the length and width, in terms of pixel number, of an image I. The standard deviation stands for the deviation degree at the gray mean for each pixel. The entropy(E) is defined as

$$E = -\sum_{i=1}^{L} P(i) \log P(i) \tag{18}$$

where L is the number of gray levels in the image, and $P(i)$ is the normalized histogram. It is used here to generally measure the mean information amount. The larger the entropy of the fused image, the richer the information extracted from the original images. The mean gradient (MG) is defined as

$$\nabla \bar{g} = \frac{\sqrt{\sum_{i=2}^{M}\sum_{j=2}^{N}(\nabla_x I^2(i,j) + \nabla_y I^2(i,j))}}{(M-1)(N-1)} \tag{19}$$

$$\begin{cases} \nabla_x I(i,j) = I(i,j) - I(i-1,j) \\ \nabla_y I(i,j) = I(i,j) - I(i,j-1) \end{cases} \tag{20}$$

The mean gradient reflects the contrast between the detailed variations of pattern on the image and the clarity of the image. The correlation coefficient (CC) is defined as

$$corr(F,A) = \frac{\sum\sum(F(i,j) - \bar{F})(A(i,j) - \bar{A})}{\sqrt{\sum\sum(F(i,j) - \bar{F})^2 \sum\sum(A(i,j) - \bar{A})^2}} \tag{21}$$

where $\bar{F}$ and $\bar{A}$ stand for the mean gray values of the fused image and original image. The correlation coefficient between the original and fused image shows similarity in small size structures between the original and synthetic images.

In Table 1, the standard deviation, entropy, mean gradient and correlation coefficient of the contourlet-based false color fusion method are all greater than those of false color mapping method for each color channel. Hence the contourlet-based method is more effective.

5 Conclusion

In this paper, a new contourlet-based false color fusion method for two different band SAR images was presented. Contourlets are a newly developed multi-scale geometrical analysis tool widely used in image processing field due to their flexible multiresolution, local and directional expansion for images. The edge information measurement based fusion rule was performed to synthesize the complementary intrinsic geometrical structures of different band SAR images. And the hybrid high boost filtered false color fusion can enhance the spectral resolution of SAR images while the spatial resolution is perfectly preserved. The color translated from gray information is conveniently perceived, recognized and classified by human visual system.

An experiment study was conducted by applying the proposed method and the false color mapping method, to the fusion of Ku and L band SAR images. The comparison of the fused image and the evaluation parameters show that the proposed method provided better results than the con-

Table 1 The quantitative evaluation of the fused results

Method	Color channel	STD	E	MG	CC
The proposed method	R	75.3576	5.2406	54.9247	0.6949
	G	75.6482	5.2630	55.9230	0.7626
	B	77.0193	5.2901	55.1361	0.8083
The false color mapping method	R	70.6619	5.1124	49.1224	0.5945
	G	71.8443	5.1779	50.4386	0.6470
	B	72.7011	5.1583	48.7922	0.6973

ventional ones, both visually and quantitatively.

Acknowledgement

The authors would like to acknowledge the 38th Research Institute of CETC for affording the multi-band SAR images.

References

1 Jiao Li-Cheng, Tan Shan. Development and prospect of image multiscale geometric analysis. *Acta Electronica Sinica*, 2003, **31**(12A): 1975∼1981(in Chinese)

2 Do M N, Vetterli M. Contourlets. In: *Beyond Wavelets*. Stoeckler J and Welland G V, Eds. New York, USA: Academic Press, 2002: 1∼27

3 Do M N. Directional Multiresolution Image Representations[Ph.D. dissertation], Swiss Federal Institute of Technology, 2001

4 Ramin E, Hayder R. Image denoising using translation-invariant contourlet transform. In: Proceedings of 2005 IEEE International Conference on Acoustics, Speech, and Signal Processing. IEEE, 2005. 557∼560

5 Vetrivelan P, Subha R R. Wavelet based contourlet transform for image compression. In: Processings of International Conference of Cognition and Recognition. IEEE, 2005. 915∼919

6 Chen D P, Li Q. The use of complex contourlet transform on fusion scheme. *Transaction on Engineering, Computing and Technology*, 2005, **7**: 342∼347

7 Do M N, Vetterli M. Contourlets: a directional multiresolution image representation. In: Proceedings of IEEE 9th International Conference of Image Processing. IEEE, 2002. 357∼360

8 Do M N, Vetterli M. The contourlet transform: an efficient directional multresolution image representation. *IEEE Transactions on Image Processing*, 2005, **14**(12): 2091∼2106

9 Zheng Y A, Zhu C S, Song J S, Zhao X H. Fusion of multiband SAR images based on contourlet transform. In: Proceedings of the 2006 IEEE International Conference on Information Acquisition. IEEE, 2006. 420∼424

10 Zhao W, Mao S Y. Pixel-based image fusion with false color mapping. In: Proceedings of 2003 SPIE Image Processing and Pattern Recognition in Remote Sensing. SPIE, 2003. 140∼149

11 Li X C, Chen J. An efficient method to evaluate fusion performance of remote sensing image. In: Proceedings of the 4th International Symposium on Multispectral Image Processing and Pattern Recognition: Image Analysis Techniques. SPIE, 2005. **6044**: 138∼148

12 Shi W Z, Zhu C Q, Yang C Y, Yang X M. Multi-band wavelet for fusing SPOT panchromatic and multispectral images. *Photogrammetric Engineering and Remote Sensing*, 2003, **69**(5): 513∼520

ZHENG Yong-An Ph. D. candidate at Xi′an Research Institute of High-tech. He received his M. S. degree from Xi′an Research Institute of High-tech in 2004. His research interest covers remote sensing image processing and multisensor information fusion. Corresponding author of this paper. E-mail: zyaomeng@163.com

SONG Jian-She Professor. He received his Ph. D. degree from Northwestern Polytechnical University in 2001. His research interest covers remote sensing image processing and information system analysis. E-mail: jssong@pub.xaonline.com

ZHOU Wen-Ming Ph. D. candidate at Xi′an Research Institute of High-tech. He received his M. S. degree from Xi′an Research Institute of High-tech in 2004. His research interest covers remote sensing image and radar signal processing. E-mail: zhouwenming7012@sohu.com

WANG Rui-Hua Master student at Xi′an Research Institute of High-tech. She received her B. S. degree from Shannxi Normal University in 2005. Her research interest covers remote sensing image and radar signal processing. E-mail: wrh_1208@163.com